A soluble theory for the density of states of a spatially disordered system

1989 J. Phys.: Condens. Matter 1 1753

(http://iopscience.iop.org/0953-8984/1/9/018)

J. Phys.: Condens. Matter 1 (1989) 1753–1771. Printed in the UK

A soluble theory for the density of states of a spatially disordered system

Martyn D Winn and David E Logan
Physical Chemistry Laboratory, University of Oxford, South Parks Road, Oxford OX1 3QZ, UK

Received 21 July 1988

Abstract. From an exact theory presented in a previous paper, we develop systematically an approximate single-site description for the density of states of a random tight-binding model characterised by quenched liquid-like disorder. The resultant theory is formally equivalent to the single super-chain approximation (SSCA) introduced by Wertheim in the context of classical dielectric theory. We show that the SSCA is equivalent to the effective-medium approximation (EMA) of Roth, and further, for a simple choice of the pair distribution function, that the SSCA/EMA is formally equivalent to the mean spherical approximation of liquid-state theory. For a Yukawa transfer matrix element, an analytic solution of the SSCA/EMA is derived and its predictions discussed. A comparison is also made with the Matsubara–Toyozawa approximation to illustrate the effect of including the structural characteristics of the system. Finally, we discuss some straightforward extensions of the theory including incorporation of site-diagonal disorder, multiple-hopping processes, and the effects of orbital overlap.

1. Introduction

In previous years, numerous theories have been proposed for the density of states of spatially disordered systems, which incorporate at some level of approximation the structural characteristics of the disordered medium. In a recent paper (Logan and Winn 1988, to be referred to as I) we have given a formally exact description of the ensemble-averaged Green functions for an off-diagonally disordered tight-binding model characterised by quenched liquid-like disorder. In this paper we develop systematically an approximate single-site theory for the averaged Green functions. As in I we draw on parallels from classical dielectric theory, and the single-site theory given here is formally identical to the single super-chain approximation (SSCA) of Wertheim (1973) in the dielectric context. In § 2 we show in addition that the SSCA is equivalent to the effective-medium approximation (EMA) of Roth (1974a, b, 1975, 1976), which has been studied numerically and is usually regarded as the best single-site theory for the density of states.

To our knowledge, however, no analytical solutions to the EMA equations have been given. For a simple choice of the pair distribution function, we show in § 2 that the SSCA/EMA is further equivalent to the much-studied mean spherical approximation of liquid-state theory for the pair distribution function of a classical liquid (Lebowitz and Percus 1966). Analytical solutions to the latter problem are known from which, for a variety of transfer matrix elements, we can in turn obtain corresponding solutions to the SSCA/EMA for the density of states of a spatially disordered tight-binding model. An application of

0953-8984/89/091753 + 19 $02.50

this is given in § 3 for the case of a Yukawa transfer matrix element, and the resulting density of states is discussed in some detail in § 4. In the final section we discuss some generalisations of the theory, including incorporation of site-diagonal disorder (which is simple), extension to include the multiple-hopping processes omitted in any single-site theory, and the inclusion of overlap effects, which is also straightforward. We begin by summarising the basic equations given in I.

For a given centre-of-mass configuration, the model system we consider is specified by a tight-binding Hamiltonian

$$H = \sum_i \varepsilon_i c_i^+ c_i + \sum_{ij}{}' V_{ij}\, c_i^+ c_j \tag{1}$$

where c_i^+ (c_i) is a creation (annihilation) operator for the one-electron (or exciton) state centred on site i, which has centre-of-mass position $\boldsymbol{R}_i$. ε_i is the zero-order site energy, V_{ij} is the transfer matrix element between sites i and j, and the prime in the second summation excludes the case $i = j$. In general, the ε_i may be treated as independent random variables with a given probability distribution, $P(\varepsilon_i)$, but in most of this paper we will consider the case of pure off-diagonal disorder, $\varepsilon_i = \varepsilon_0$ for all i; without loss of generality we can set $\varepsilon_0 = 0$. For single-site theories, such as the one developed in this paper, extension to include site-diagonal disorder is straightforward, and we will briefly discuss this case in the final section. We also assume that V_{ij} is a function only of the relative site centre-of-mass separation: $V_{ij} \equiv V(\boldsymbol{R}_i - \boldsymbol{R}_j)$.

In I, we showed that the configurationally averaged diagonal Green function, $\bar{G}(z) = [z - S(z)]^{-1}$ (where the self-energy, $S(z)$, is thus defined), satisfies the following exact equations:

$$z\bar{G}(z) = 1 + \rho[\bar{G}(z)]^2 \int \mathrm{d}(2)\, H(12)\, V(21) \tag{2}$$

$$H(12) = C(12) + \rho\bar{G}(z) \int \mathrm{d}(3)\, H(13)\, C(32). \tag{3}$$

Combining these, we obtain the result

$$z\bar{G}(z) = 1 + \rho[\bar{G}(z)]^2 \int \frac{\mathrm{d}\boldsymbol{k}}{(2\pi)^3} \frac{\hat{C}(\boldsymbol{k})\hat{V}(\boldsymbol{k})}{1 - \rho\bar{G}(z)\hat{C}(\boldsymbol{k})}. \tag{4}$$

In these equations, $i = 1, 2, \ldots$ as the argument of a function is shorthand for $\boldsymbol{R}_i$, and $\mathrm{d}(i) \equiv \mathrm{d}\boldsymbol{R}_i$; for example, $H(12) \equiv H(\boldsymbol{R}_1 - \boldsymbol{R}_2)$. $z = E + \mathrm{i}\eta$ is the energy (η is a positive infinitesimal), ρ is the number density of sites, and the Fourier transform, $\hat{f}(\boldsymbol{k})$, of a function $f(\boldsymbol{R})$ is defined by

$$\hat{f}(\boldsymbol{k}) = \int \mathrm{d}\boldsymbol{R}\, f(\boldsymbol{R}) \exp(-\mathrm{i}\boldsymbol{k}\cdot\boldsymbol{R}). \tag{5}$$

The function $H(12)$ is related to the configurationally averaged off-diagonal Green function, $\bar{G}(12)$, by

$$\bar{G}(12) = \bar{G}(z)H(12)\bar{G}(z). \tag{6}$$

As discussed in I, $\bar{G}(12)$ and $C(12)$ are defined in terms of composite graphs consisting of a continuous, directed chain of V_{ij} bonds, with additional connectors from the s-particle structural distribution functions $g_s(1 \ldots s)$. Specifically, $\bar{G}(12)$ is the sum of all chain-continuous composite graphs containing two root points (RP) at the end stages

(labelled 1 and 2), a factor of ρ for each field point (FP), no one-articulation points (1-AP), and a factor of $\bar{G}(z)$ associated with each stage. Similarly, $C(12)$ is the sum of all chain-continuous composite graphs containing two RP at the end stages, a factor of ρ for each FP, no 1-AP, no one-chain bridge points (1-BP), a factor of $\bar{G}(z)$ associated with each interior stage, and a factor of unity associated with each end stage. Expressed in renormalised form as above, the function $C(12)$ is said to be strongly irreducible in the sense that it lacks both 1-BP and 1-AP; in consequence, the z dependence of $C(12)$ is implicit in the $\bar{G}(z)$ dependence of the function, so that the right-hand side of the self-consistency equation (4) does not depend explicitly on z. A stage is defined as a contact of the V-chain with a point. In any graph, the FP are integrated over whereas the RP are not. For the definitions of 1-AP and 1-BP, and for the derivation of the above equations, the reader is referred to I. Figure 1 shows all composite graphs in $C(12)$ with a chain-continuous component of up to four V_{ij} bonds (the RP are denoted by open circles and the V_{ij} bonds by full lines).

Although we have an algorithm for the construction of all graphs in $C(12)$ (see I and Wertheim 1973), we do not have an exact closed expression for this function. Therefore, we must resort to approximation. Equation (3) provides a single relation between the two unknowns $C(12)$ and $H(12)$. To obtain a closed solution for $C(12)$ and $H(12)$, a second, so-called closure, relation between these functions must be provided via some suitable approximation. We note that equation (3) for $H(12)$ is analogous to the Ornstein–Zernike (OZ) equation for the pair distribution function $h_2(12)$ $(=g_2(12)-1)$ of a fluid, with $H(12)$ replacing $h_2(12)$, $C(12)$ replacing the direct correlation function $c_2(12)$, and with $\rho\bar{G}(z)$ replacing ρ. There is a vast literature devoted to obtaining a suitable closure relation to the OZ equation of liquid-state theory (see for example Hansen and McDonald 1986). If, by exploiting analogies in conventional liquid-state theory, we could obtain a suitable closure relation to equation (3), then we could determine $H(12)$, and hence $\bar{G}(z)$ via equation (2). This approach is different to that used in many theories for $\bar{G}(z)$ (e.g. Ishida and Yonezawa 1973, Movaghar and Miller 1975, Katz and Rice 1972). Here we insist that the OZ form, equation (3), for $H(12)$ is maintained and we make approximations to the basic irreducible unit $C(12)$. However, in other theories approximations are often made directly to $H(12)$ without the OZ form being maintained, as discussed in I. As well as the increased clarity provided by the present approach, we feel that breaking the OZ form may have more serious implications, one of which will be mentioned in § 4.

In the next section we derive an approximate closure relation to supplement equation (3), by the use of the single super chain approximation (SSCA), originally suggested by Wertheim (1973) in his work on the classical dielectric theory of non-polar fluids, to which the present problem is formally analogous, as discussed in I. As we will show, the SSCA is equivalent to the effective-medium approximation (EMA) of Roth (1974a, b, 1975, 1976—see also Yonezawa *et al* 1975). To the best of our knowledge, no analytic solutions to the EMA equations have been given. Such solutions can, however, be obtained by exploiting some results of liquid-state theory. This is straightforward in the SSCA formulation, since this is based on $H(12)$ and $C(12)$ which are analogous respectively to the pair distribution function h_2 and the direct correlation function c_2, of liquid-state theory; in contrast, such analogies are not entirely obvious in the EMA formulation. In particular, if we take the pair distribution function, $g_2(R)$, between sites to be a simple step function, $\theta(R-\sigma)$, then the SSCA is formally equivalent to the mean spherical approximation (MSA) of liquid-state theory (see e.g. Hansen and McDonald 1986). In the context of dielectric theory, the formal correspondence between the SSCA (with

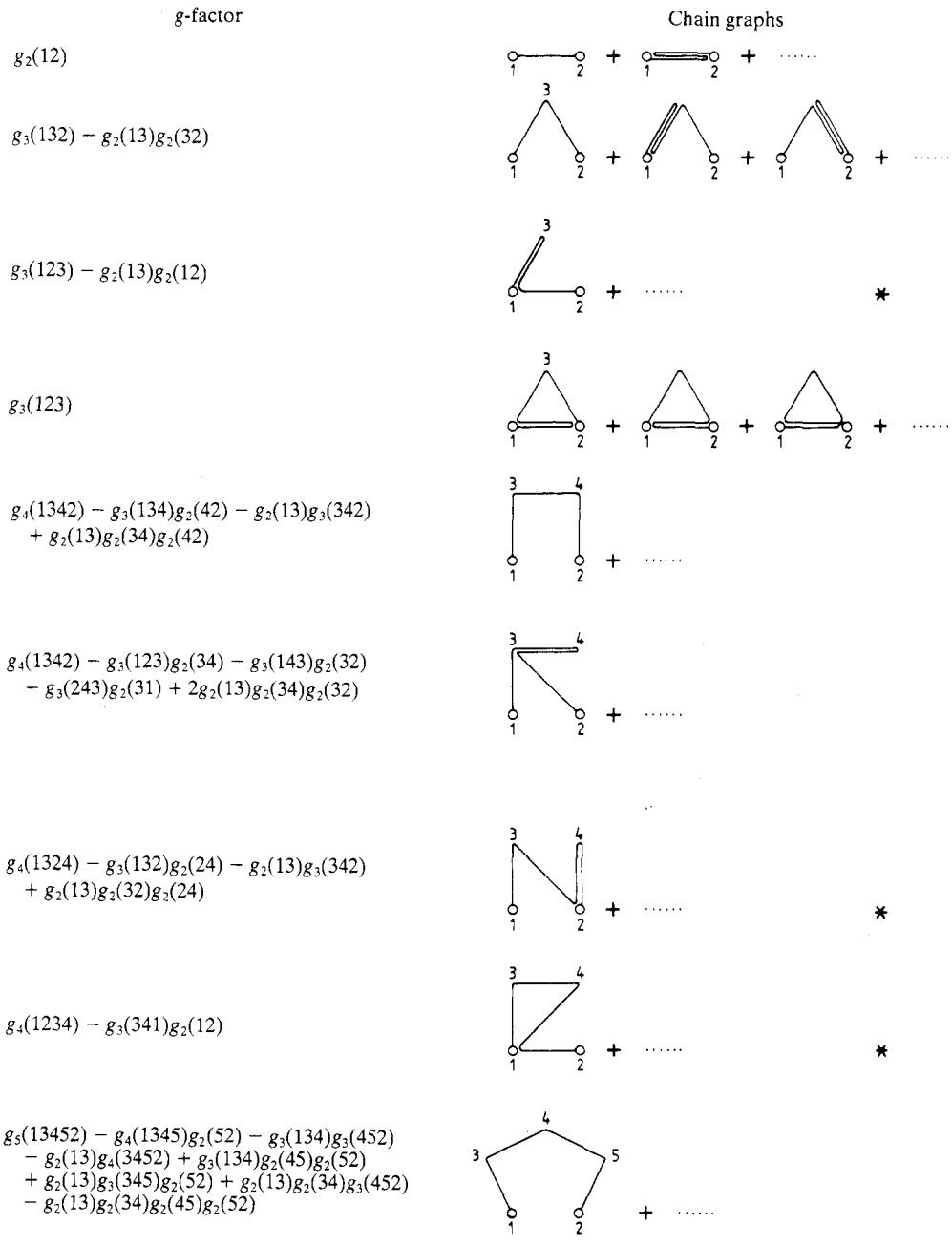

Figure 1. All composite, renormalised (1-AP-free) graphs contributing to $C(12)$ with a chain-continuous component of up to four V_{ij} bonds. A factor of ρ is associated with each FP, and a factor of $\bar{G}(z)$ (1) is associated with each interior (end) stage. To the rows with asterisks add the 'mirror image' obtained by interchanging 1 and 2 in both columns.

$g_2(R) = \theta(R - \sigma)$) and the MSA for a fluid of permanent dipolar molecules (Wertheim 1971) has been used by Wertheim (1973) to obtain analytic solutions for the renormalised static polarisability and hence the static dielectric constant of a non-polar fluid. An analytical continuation of Wertheim's results into the complex energy or frequency plane yields the density of states appropriate to the case of an angle-dependent dipolar transfer matrix element, and also the frequency-dependent renormalised polarisability and dielectric constant of a non-polar fluid. The latter have been discussed by Høye and Olaussen (1982) and Chandler *et al* (1982), although the methodology of these papers differs somewhat from that of Wertheim, and is based on a path integral approach to the statistical mechanics of a quantum polarisable fluid which has been studied extensively over the past few years (see e.g. Høye and Stell 1981, Thompson *et al* 1982, Schweizer and Chandler 1983, Logan 1984, Hall and Wolynes 1985, Schweizer 1986).

In § 3 of this paper, and for the case of a Yukawa transfer matrix element, we exploit the correspondence between the SSCA/EMA and the MSA, together with an analytic solution to the MSA for the pair distribution function of a classical hard-sphere fluid with particles interacting via a Yukawa potential (Waisman 1973, Høye and Stell 1976, Høye *et al* 1976, Høye and Blum 1977). We obtain thereby a simple quartic equation for the self-energy, which can be solved to yield $\bar{G}(z)$ and hence the density of states. In § 4 we analyse the results and compare them with the Matsubara–Toyozawa approximation (MTA) (Matsubara and Toyozawa 1961) for the perfectly random fluid ($g_2(R) = 1$).

2. Single super-chain approximation

Expressing the first graph in $C(12)$ (see figure 1) explicitly, we can write

$$C(12) = g_2(12)V(12) + T(12) \tag{7}$$

where $T(12)$ is thus defined. We now obtain an approximate $T(12)$ (denoted by $T^0(12)$) by neglecting certain classes of graphs. First, we confine ourselves to a single-site description. As discussed in I, a general single-site theory is specified by two conditions: (i) the $s \geqslant 3$-body liquid distribution functions, $g_s(12 \ldots s)$, are approximated by the Kirkwood superposition approximation; (ii) only single-site graphs are retained in $T(12)$, meaning those renormalised graphs (free of 1-AP) in which only a single stage is associated with any point. We expect a single-site theory to lead to a better description of the density of states at higher number densities (see e.g. Movaghar and Miller 1975), since at lower densities multiple hopping between pairs of sites will become important, and such processes are omitted in any single-site theory. A typical single-site graph in $T(12)$ will therefore consist of an open polygon of $s - 1$ $g_2(ij)V(ij)$ bonds connecting s points ($s \geqslant 3$) with enough interior $h_2(ij) = g_2(ij) - 1$ connectors to render the graph strongly irreducible. We now make the further approximation of neglecting all graphs with crossing interior $h_2(ij)$ bonds. The lack of crossing $h_2(ij)$ bonds means that all graphs retained in the resultant $T^0(12)$ must possess an $h_2(12)$ bond between the RP, since the absence of such would otherwise guarantee at least one 1-BP in each graph in $T^0(12)$. The presence of the $h_2(12)$ bond is, however, sufficient to ensure that the graphs in $T^0(12)$ are indeed strongly irreducible. If therefore we write

$$T^0(12) = h_2(12)F^0(12) \tag{8}$$

then $F^0(12)$ is the sum of all graphs consisting of an open polygon of $s - 1$ $g_2(ij)V(ij)$ bonds connecting s points ($s \geqslant 3$) with any combination of $h_2(ij)$ bonds connecting within

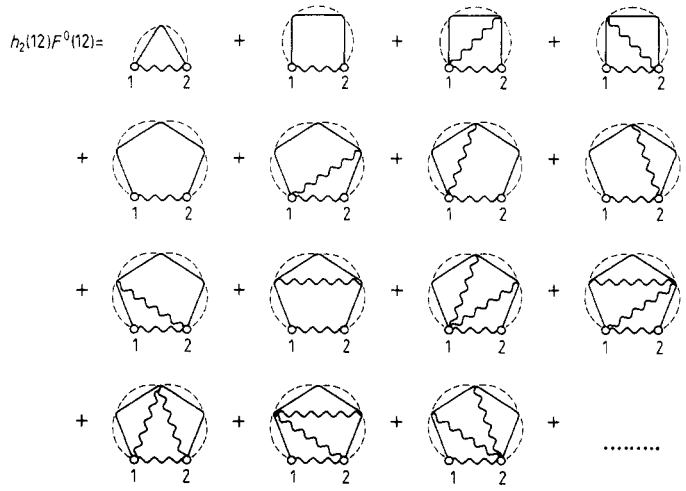

Figure 2. All composite, renormalised graphs contributing to $h_2(12)F^0(12)$ with a chain of up to four $g_2(ij)V(ij)$ bonds. Broken line between points i and j denotes a $g_2(ij)$ bond, and wavy line between points i and j denotes a short-ranged $h_2(ij)$ bond. A factor of $\rho\bar{G}(z)$ (1) is associated with each FP (RP).

the periphery of the polygon such that none cross each other. The approximate $C(12)$ is thus given by

$$C^0(12) = g_2(12)V(12) + h_2(12)F^0(12). \tag{9}$$

Figure 2 shows all the graphs in $h_2(12)F^0(12)$ with up to four $g_2(ij)V(ij)$ bonds. The corresponding graphs in $F^0(12)$ are obtained simply by deleting the $h_2(12)$ bond between the RP 1 and 2, and those in $C^0(12)$ are obtained by adding the single graph consisting of a full and a broken line between 1 and 2, representing $g_2(12)V(12)$.

All graphs in $F^0(12)$ contain at least one 1-BP, and at each 1-BP the cut is unique, i.e. the maximal and minimal cuts (see I) are identical. By making cuts at all the 1-BP of the graphs in $F^0(12)$ we arrive at the expression

$$F^0(12) = \rho\bar{G}(z)\int \mathrm{d}(3)\, C^0(13)C^0(32) + [\rho\bar{G}(z)]^2 \times \iint \mathrm{d}(3)\mathrm{d}(4)C^0(14)C^0(43)C^0(32) + \ldots$$

$$= H^0(12) - C^0(12) \tag{10}$$

where $H^0(12)$ is related to $C^0(12)$ by

$$H^0(12) = C^0(12) + \rho\bar{G}(z)\int \mathrm{d}(3)\, H^0(13)C^0(32) \tag{11}$$

in an analogous manner to equation (3). Combining equations (9) and (10) gives

$$g_2(12)C^0(12) = g_2(12)V(12) + h_2(12)H^0(12). \tag{12}$$

This is the central result of the SSCA. Equation (12) is the desired approximate closure condition to equation (11), which allows us to determine $H^0(12)$ in terms of $\bar{G}(z)$;

equation (2), with $H(12)$ replaced by $H^0(12)$, then gives a self-consistency equation for $\bar{G}(z)$. Note that equation (12) can also be written as

$$H^0(12) = \bar{C}^0(12) + g_2(12)S^0(12) \tag{13}$$

where $\bar{C}^0(12) = g_2(12)V(12)$ and $S^0(12) = H^0(12) - C^0(12)$. This is equation (25) of I for the case of the SSCA, and this is the form in which several alternative approximate single-site theories for $\bar{G}(z)$ were discussed and compared.

The EMA of Roth (1974a, b, 1975, 1976) can be summarised by the following equations in $\boldsymbol{k}$-space (see for example, equations (3.4)–(3.6) of Whitelaw and McLaughlin (1979)):

$$z\bar{G}(z) = 1 + \bar{G}(z) \int \frac{\mathrm{d}\boldsymbol{k}}{(2\pi)^3} M(\boldsymbol{k})G(\boldsymbol{k})\hat{V}(\boldsymbol{k}) \tag{14}$$

$$G(\boldsymbol{k}) = \rho/\{[\bar{G}(z)]^{-1} - \rho M(\boldsymbol{k})\} \tag{15}$$

$$M(\boldsymbol{k}) = \tilde{V}(\boldsymbol{k}) + \int \frac{\mathrm{d}\boldsymbol{k}'}{(2\pi)^3} h_2(\boldsymbol{k} - \boldsymbol{k}')[M(\boldsymbol{k}')]^2 G(\boldsymbol{k}'). \tag{16}$$

Here, $\tilde{V}(\boldsymbol{k})$ is the Fourier transform of $g_2(12)V(12)$, and $G(\boldsymbol{k})$ is the Fourier transform of

$$\left\langle \sum_{ij} G_{ij}\delta(\boldsymbol{R}_i - \boldsymbol{R})\delta(\boldsymbol{R}_j - \boldsymbol{R}') \right\rangle = \rho\bar{G}(z)\delta(\boldsymbol{R} - \boldsymbol{R}') + \rho^2\bar{G}(\boldsymbol{R} - \boldsymbol{R}').$$

In fact, equations (14), (15) and (16) are equivalent to equations (2), (11) and (12), as can be seen by Fourier-transforming the latter and identifying $M(\boldsymbol{k})$ with $\hat{C}^0(\boldsymbol{k})$ and $G(\boldsymbol{k})$ with $\rho\bar{G}(z)\hat{H}^0(\boldsymbol{k})/\hat{C}^0(\boldsymbol{k})$. But, although the SSCA and the EMA are equivalent, we feel that an approach via the SSCA formalism may be preferable, since the problem of solving an OZ-type equation with an appropriate closure condition is common, and has been extensively studied. In particular, the SSCA formalism allows us to exploit analogies to more conventional problems in liquid-state theory, as we will discuss below.

To proceed further we must solve equations (11) and (12) for $H^0(12)$ and $C^0(12)$, with a given transfer matrix element, $V(12)$. This requires a specification of $g_2(R)$, and in general these equations may be solved numerically with a pair distribution function obtained, for example, from experimental neutron scattering studies on the system of interest. For simplicity, we here consider a simple step function $g_2(R)$, corresponding to the low-density limit of a hard-sphere fluid with hard-sphere diameter σ, i.e.

$$g_2(R) = \theta(R - \sigma) \tag{17}$$

where θ is the unit step function. We also assume that the transfer matrix element $V(12)$ (and hence $H^0(12)$ and $C^0(12)$) is a function only of $R = |\boldsymbol{R}_1 - \boldsymbol{R}_2|$. With equation (17), the SSCA/EMA closure condition, equation (12), reduces simply to

$$H^0(R) = 0 \qquad :R < \sigma \tag{18a}$$

$$C^0(R) = V(R) \qquad :R > \sigma. \tag{18b}$$

Within the Kirkwood superposition approximation, and for any choice of $g_2(R)$ which vanishes inside a hard core, equation (18*a*) is exact since $H^0(R)$ will always contain a $g_2(R)$ factor. The essential approximation in this model is thus equation (18*b*).

We now note the similarity between the OZ analogue equation (11), with the closure

conditions (18), and the familiar MSA of liquid-state theory (Lebowitz and Percus 1966) defined by

$$\tilde{h}_2(R) = c_2(R) + \rho \int \mathrm{d}\boldsymbol{R}' \tilde{h}_2(|\boldsymbol{R}-\boldsymbol{R}'|)c_2(R') \tag{19}$$

$$\tilde{h}_2(R) = -1 \qquad :R < \sigma \tag{20a}$$

$$c_2(R) = -\beta\varphi(R) \qquad :R > \sigma. \tag{20b}$$

Here, $\tilde{h}_2(R)$ ($c_2(R)$) is the total (direct) correlation function for a classical fluid of particles interacting pairwise-additively via the pair potential $U(R)$ given by

$$U(R) = \begin{cases} \infty & :R < \sigma \\ \varphi(R) & :R > \sigma \end{cases}$$

where $\varphi(R)$ is a given function; $\beta = (kT)^{-1}$ is the inverse temperature. Equation (19) is the usual OZ equation, equation (20*a*) is the exact hard-core condition, and equation (20*b*) is the characteristic approximation of the MSA. The MSA was first solved by Waisman and Lebowitz (1970) for the restricted primitive model of a 1 : 1 electrolyte in which $\varphi(R)$ is of Coulombic form. Wertheim (1971) solved the MSA for a fluid of hard spheres with permanent point dipoles, and Waisman (1973) gave the solution when $\varphi(R)$ has a Yukawa form. These early solutions used Laplace-transform techniques similar to those employed by Wertheim (1963) in solving the Percus–Yevick equation for a one-component hard-sphere fluid. A more general technique is based upon a Wiener–Hopf factorization of the OZ equation, as introduced by Baxter (1968), and Høye and Blum (1977) have solved the MSA by this method when $\varphi(R)$ is given by an arbitrary number of Yukawa interactions. Smith (1979) has given the method of solution for $\varphi(R)$ of the form

$$\sum_{n=N}^{M} \varphi_n r^{-n} \mathrm{e}^{-\mu r}$$

and Perram (1983) has considered the case of an arbitrary $\varphi(R)$ of finite range.

As discussed in § 1, equation (11) is formally equivalent to the OZ equation, (19). Equations (18*b*) and (20*b*) are also formally equivalent, with $V(R) \leftrightarrow -\beta\varphi(R)$, but the hard-core closure condition on $\tilde{h}_2(R)$ (equation (20a)) is clearly slightly different from that for $H^0(R)$ (equation (18*a*)). However, the solution to the OZ equation (19) with a closure condition

$$\tilde{h}_2(R) = 0 \qquad :R < \sigma \tag{21}$$

is usually no more difficult to obtain than that for the closure (20*a*). If, therefore, the MSA can be solved analytically for a given $\varphi(R)$ with the closure conditions (20*b*) and (21), then we can find immediately the solution of equations (11) and (18) relevant to the present problem.

3. Averaged Green function for Yukawa transfer matrix element

It is known that an exponential or modified exponential transfer matrix element of the general form $V(R) = -V_0 f(R) \exp(-\alpha R)$ is appropriate to describe several problems of physical interest, such as electronic transport in tightly bound bands of certain liquid

metals and alloys, the impurity band of a doped semiconductor, and triplet electronic excitons in the impurity band of isotopically mixed organic solids. The function $f(R)$ is usually chosen as either a constant or a polynomial in R, but for simplicity of analysis we here consider the case where $f(R) = R^{-1}$, corresponding to the Yukawa transfer matrix element

$$V(R) = -(V_0/R)\exp(-\alpha R). \tag{22}$$

Waisman (1973) has solved analytically the MSA of liquid-state theory (equations (19) and (20)) for the case of a Yukawa $\varphi(R)$, and Høye *et al* (1976) have pointed out that changing the core condition on $\tilde{h}_2(R)$ from equation (20*a*) to (21) results simply in the coefficients a and b of Waisman's solution being set to zero. With an appropriate modification of Waisman's (1973) results, we can thus obtain directly an analytic solution to the SSCA/EMA (equations (11) and (18)) for a Yukawa transfer matrix element, and with $g_2(R) = \theta(R - \sigma)$. Outside the core ($R > \sigma$), $C^0(R)$ is given by equation (18*b*), and inside the core the R-dependence of $C^0(R)$ is given by

$$C^0(R) = -S(z)(1-\exp(-\alpha R))/\alpha R + (S(z))^2(\cosh(\alpha R)-1)/2V_0\alpha^2 R \qquad :R<\sigma. \tag{23}$$

The function $S(z) \equiv S(\bar{G}(z))$ is related to $H^0(R)$ by

$$S(z) = \rho\bar{G}(z)\int H^0(R)V(R)\,\mathrm{d}\boldsymbol{R} \tag{24a}$$

and is given as a function of $\bar{G}(z)$ by solution of

$$4\pi\rho\bar{G}(z)y_0^2 = 2S(z)\alpha + (S(z))^2V_0^{-1} \tag{24b}$$

where $y_0 \equiv y_0(S(z))$ is given by

$$y_0 = \left(-V_0\exp(-\alpha R) - RC^0(R)\right)_{R=\sigma^-}. \tag{24c}$$

Substituting equation (24*a*) into equation (2) yields

$$z\bar{G}(z) = 1 + \bar{G}(z)S(z) \tag{25}$$

and so we identify $S(z)$ as the self-energy, a determination of which yields $\bar{G}(z)$ and hence the density of states. From equations (24*b*, *c*) and (23), we see that $S(z)$ satisfies the quartic equation

$$\begin{aligned}4\pi\rho\bar{G}(z)\{&-V_0\exp(-\alpha\sigma) + (S(z)/\alpha)\\ &\times(1-\exp(-\alpha\sigma)) - [(S(z))^2/2V_0\alpha^2](\cosh(\alpha\sigma)-1)\}^2\\ &= 2S(z)\alpha + (S(z))^2V_0^{-1}.\end{aligned} \tag{26}$$

The system of interest has two length scales—the hard-sphere diameter σ, and the effective Bohr radius $a_H = \alpha^{-1}$—either of which can be chosen as the standard unit of length. Since we will be interested partly in liquid-like densities, we follow the norm of liquid-state theory and choose σ as the basic length unit. We define

$$V_0^* = V_0/\sigma$$

(which has dimensions of energy), and the reduced (dimensionless) variables

$$\rho^* = \rho\sigma^3 \qquad \alpha^* = \alpha\sigma \equiv \sigma/a_H \qquad \tilde{z} = z/V_0^*. \tag{27a}$$

We also define a reduced self-energy, $\tilde{S}(z)$, and a reduced averaged diagonal Green function, $\tilde{G}(z)$, by

$$\tilde{S}(z) = S(z)/V_0^* \qquad \tilde{G}(z) = V_0^* \bar{G}(z). \tag{27b}$$

Equations (26) and (25) thus simplify to

$$4\pi\rho^*\tilde{G}(z)\{-\exp(-\alpha^*) + (\tilde{S}(z)/\alpha^*)(1-\exp(-\alpha^*)) - [(\tilde{S}(z))^2/2\alpha^{*2}](\cosh(\alpha^*)-1)\}^2$$
$$= 2\alpha^*\tilde{S}(z) + (\tilde{S}(z))^2 \tag{28}$$

and

$$\tilde{G}(z) = (\tilde{z} - \tilde{S}(z))^{-1}. \tag{29}$$

Finally, substituting $\tilde{G}(z)$ (as given by equation (28)) into equation (29), and rearranging, gives

$$\tilde{z} = \frac{4\pi\rho^*}{\tilde{S}(z)(2\alpha^* - \tilde{S}(z))} \times \left(-\exp(-\alpha^*) + \frac{\tilde{S}(z)}{\alpha^*}(1-\exp(-\alpha^*)) - \frac{(\tilde{S}(z))^2}{2\alpha^{*2}}(\cosh(\alpha^*)-1)\right)^2 + \tilde{S}(z). \tag{30}$$

Solution of equations (29) and (30) yields the density of states, $D(\varepsilon)$, or the reduced density of states, $\tilde{D}(\varepsilon)$, given by

$$\tilde{D}(\varepsilon) = V_0^* D(\varepsilon) = -\pi^{-1} \lim_{\eta \to 0^+} \mathrm{Im}(\tilde{G}(\varepsilon + \mathrm{i}\eta)) \tag{31}$$

where we decompose the reduced energy, $\tilde{z}$, as

$$\tilde{z} = \varepsilon + \mathrm{i}\eta.$$

Before proceeding to a determination of the full density of states we must decide which of the four roots of equation (30), a quartic for $\tilde{S}(z)$, is physically appropriate. In the limit that $\eta \to 0$, equation (29) shows that $\tilde{S}(z)$ is complex only if $\tilde{G}(\varepsilon)$ is complex, i.e. within the band. In figure 3 we show a typical sketch of ε versus $\tilde{S}$ obtained from equation (30) for real $\tilde{S}$. The figure implies that in the energy intervals $\varepsilon_- < \varepsilon < \varepsilon_+$ and $\varepsilon < \varepsilon_L$, there are two complex values of $\tilde{S}$ which satisfy equation (30). These are therefore the energy intervals in which $\tilde{G}(\varepsilon)$ can be complex. To select the physically valid root we note that (as follows directly from the locator expansion for the diagonal Green function) $\tilde{G}(\varepsilon) \to 1/\varepsilon$ as $\varepsilon \to \pm\infty$; thus from equation (29), $\tilde{S}(\varepsilon) \to 0$ as $\varepsilon \to \pm\infty$. The physically required root of equation (30), for ε outside the band, is thus that indicated by arrows in figure 3. Assuming that $\tilde{S}(\varepsilon)$ is a continuous function of ε, this root will connect points A and B of figure 3 in the region $\varepsilon_- < \varepsilon < \varepsilon_+$, but it will be complex. Hence we can identify ε_+ and ε_- as the upper and lower band edges respectively. Within the band ($\varepsilon_- < \varepsilon < \varepsilon_+$) there will in fact be two complex-conjugate roots connecting A and B. The real part of these roots decreases monotonically from ε_+ to ε_-, and choosing the root with the negative (positive) imaginary part leads to $\tilde{D}(\varepsilon)$ ($-\tilde{D}(\varepsilon)$) or, equivalently, corresponds to the limit $\eta \to 0^+$ ($\eta \to 0^-$).

The band edges in the density of states, ε_+ and ε_-, are thus readily found from the stationary values of equation (30). In figure 4 we show the resultant band-edge

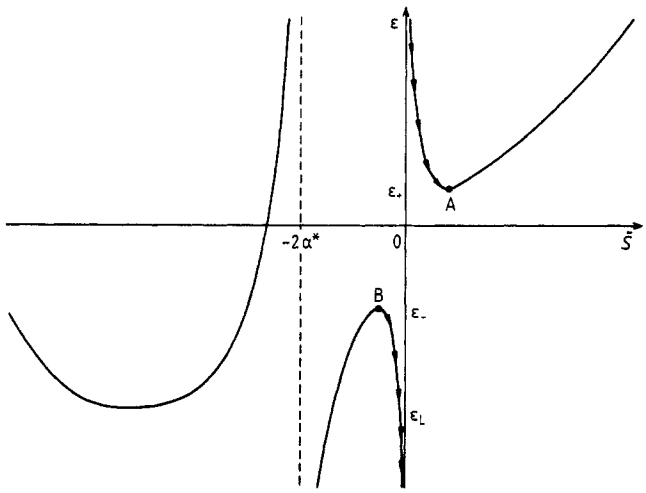

Figure 3. A typical schematic plot of ϵ against $\tilde{S}$ for real $\tilde{S}$, as obtained from equation (30).

trajectories, $\varepsilon_+(\rho^*)$ and $\varepsilon_-(\rho^*)$, as functions of ρ^* for several different values of the ratio $\alpha^* = \sigma/a_H$. For a given value of α^*, the band width increases with increasing density, as one expects, and the band becomes increasingly asymmetric. For a given ρ^*, we also see that the asymmetry in the band-edge trajectories becomes increasingly marked as we progressively diminish α^*, leading in particular to a very long low-energy tail in the density of states. In fact the figure does not capture fully the extent to which the lower band edge rapidly diminishes with decreasing α^*, and in table 1 we give ε_+

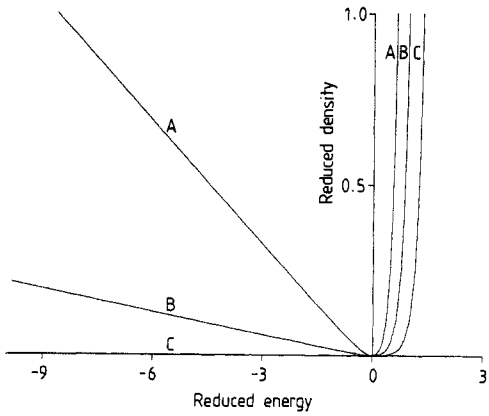

Figure 4. Upper and lower band-edge trajectories, $\varepsilon_\pm(\rho^*)$, as functions of reduced density, ρ^*, for (A) $\alpha^* = 1$, (B) $\alpha^* = 0.5$ and (C) $\alpha^* = 0.05$.

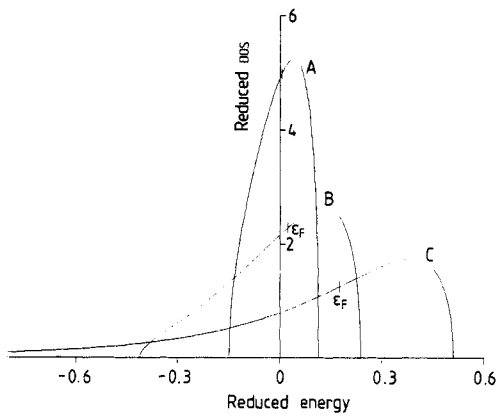

Figure 5. The reduced density of states, $\tilde{D}(\epsilon)$, for $\rho^* = 0.005$ and (A) $\alpha^* = 1$, (B) $\alpha^* = 0.5$ and (C) $\alpha^* = 0.05$.

Table 1. Upper band edges (ε_+) and lower band edges (ε_-) for several ρ^* and α^*.

ρ^*	α^*	ε_+	ε_-
0.005	1.00	0.115	−0.149
	0.50	0.239	−0.412
	0.05	0.511	−25.151
0.100	1.00	0.365	−1.008
	0.50	0.626	−4.742
	0.05	0.990	−502.125
1.000	1.00	0.642	−8.640
	0.50	0.968	−44.984
	0.05	1.359	−5020.819

and ε_- for three reduced densities, varying $\alpha^* = \sigma/a_H$ from 1 to 0.05 in each case. For $\rho^* = 0.1$, for example, we see that $\varepsilon_- \simeq -1.1$ and $\varepsilon_+ \simeq 0.37$ for $\sigma = a_H$, whereas ε_- drops to $\varepsilon_- \simeq -502$ for $a_H = 20\sigma$, with $\varepsilon_+ \simeq 0.99$. This marked increase in band width obviously reflects the increased spatial range of the transfer matrix element as $a_H = \alpha^{-1}$ is increased for a given value of σ.

4. Density of states

We can now proceed to a determination of the energy spectrum via equations (29) and (30). This is done by selecting a complex value of $\tilde{S}$, and finding the appropriate $\varepsilon = \mathrm{Re}\,\tilde{z}$ from equation (30) and the corresponding $\tilde{G}(\varepsilon)$ (and hence $\tilde{D}(\varepsilon)$) from equation (29). Obviously not all values of $\tilde{S}$ are acceptable, since Im $\tilde{z}$ determined by equation (30) must be zero. In practice, we take a value of Re $\tilde{S}$ between those values associated with points A and B in figure 3, and vary Im $\tilde{S}$ until Im $\tilde{z}$ given by equation (30) is equal to zero. The resultant $\tilde{S}$, together with the ε determined from equation (30), is inserted into equation (29) to give $\tilde{G}(\varepsilon)$, and $\tilde{D}(\varepsilon)$ is finally obtained from equation (31). It is usually obvious whether or not one has chosen the correct root of equation (30). For example, if ρ^* and α^* are such that the plot of ε against $\tilde{S}$ for real $\tilde{S}$ is as in figure 3, then for $\varepsilon_- < \varepsilon < \varepsilon_+$ choosing the wrong complex root will result in a negative $\tilde{D}(\varepsilon)$.

In figures 5–7 we plot the resultant density of states $\tilde{D}(\varepsilon)$ for the three reduced densities of table 1, $\rho^* = 0.005$ (figure 5), $\rho^* = 0.1$ (figure 6) and $\rho^* = 1$ (figure 7); and in each figure we show the predicted $\tilde{D}(\varepsilon)$ for three different values of $\alpha^* = \alpha\sigma$, namely $\alpha^* = 1.0$ (curve A), 0.5 (curve B) and 0.05 (curve C). For $\rho^* = 0.005$ and $\sigma/a_H = 1$ (curve A of figure 5) the predicted density of states is relatively symmetric about $\varepsilon = 0$; but for all cases in figures 5–7 we see that $\tilde{D}(\varepsilon)$ becomes increasingly asymmetric as $\alpha^* = \sigma/a_H$ is decreased (A → C in each figure), i.e. as the range parameter, a_H, of the transfer matrix element becomes the dominant length scale. The asymmetry is particularly pronounced for larger ρ^* and smaller α^*, and its origin has been discussed by Logan and Wolynes (1986) in terms of screening (anti-screening) of the spatial range of an effective transfer matrix element in the upper (lower) region of the band. We note also that the band-edge behaviour of the density of states, for both the upper and lower edges, has the characteristic square-root form expected for

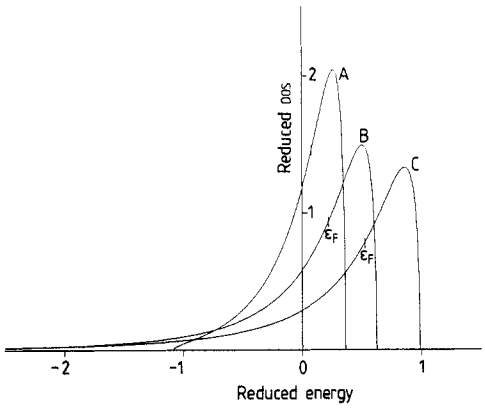

Figure 6. The reduced density of states, $\tilde{D}(\varepsilon)$, for $\rho^* = 0.1$ and (A) $\alpha^* = 1$, (B) $\alpha^* = 0.5$ and (C) $\alpha^* = 0.05$. Note the change in scale from that used in figure 5.

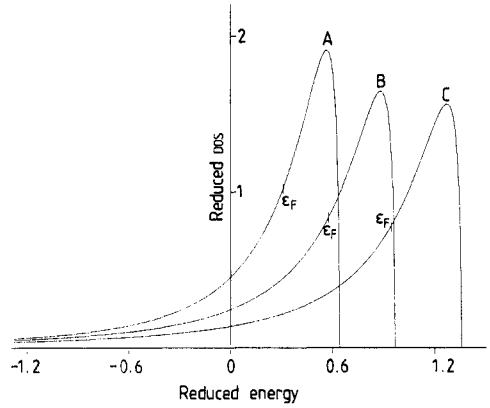

Figure 7. The reduced density of states, $\tilde{D}(\varepsilon)$, for $\rho^* = 1$ and (A) $\alpha^* = 1$, (B) $\alpha^* = 0.5$ and (C) $\alpha^* = 0.05$. Note the change in scale from those used in figures 5 and 6.

three-dimensional systems, i.e. $\tilde{D}(\varepsilon) \propto |\varepsilon_\pm - \varepsilon|^{1/2}$ for $|\varepsilon_\pm - \varepsilon| \ll 1$.

Numerical integration shows that the SSCA/EMA $\tilde{D}(\varepsilon)$ is correctly normalised to unity. This is also true of the MTA density of states for a perfectly random system. In both cases (SSCA/EMA and MTA) the OZ analogue equation (3) relating $H(12)$ to $C(12)$ is correctly preserved. In contrast, however, the OZ form of equation (3) is broken in the approximate single-site theories of Movaghar and Miller (1975) (MM) and Ishida and Yonezawa (1973) (IY), as discussed in I. Movaghar and Miller (1975) note that in both the MM and IY theories, the density of states is not correctly normalised. These results suggest that one effect of breaking the OZ form of equation (3) may be to violate the normalisation condition on $\tilde{D}(\varepsilon)$. If this is correct, then for any approximate single-site theory in which the OZ form of equation (3) is broken, a determination of the Fermi energy, the density of states at the Fermi level, and in consequence electronic transport properties in a delocalised regime, may not always be wholly reliable.

The Fermi energy ε_F, is determined by

$$\int_{\varepsilon_-}^{\varepsilon_F} \tilde{D}(\varepsilon)\, d\varepsilon = n/2$$

where n is the mean number of electrons per atom. For a half-filled band ($n = 1$), ε_F is marked in figures 5–7 and is found always to be blue-shifted from $\varepsilon = 0$, with both ε_F and $\varepsilon_F/\varepsilon_+$ increasing monotonically as ρ^* (α^*) is progressively increased (decreased) for fixed α^* (ρ^*). This emphasises the fact that although the low-energy tail in the spectrum becomes increasingly pronounced as ρ^* (α^*) is increased (decreased), the density of states there is small and the majority of states are in the upper half-band. For three fixed values of ρ^*, the α^* dependence of the density of states at the Fermi level, $\tilde{D}(\varepsilon_F)$, is shown in figure 8(a); and for three values of α^*, the ρ^* dependence of $\tilde{D}(\varepsilon_F)$ is shown in figure 8(b). For $\alpha^* \leqslant 0.5$ and $\rho^* \geqslant 0.1$, it is clear that $\tilde{D}(\varepsilon_F)$ is insensitive to both ρ^* and α^*, but there is a significant dependence of $\tilde{D}(\varepsilon_F)$ on ρ^* and α^* for smaller (larger) values of ρ^* (α^*). Note also that the density domain in which $\tilde{D}(\varepsilon_F)$ is sensitive to variations in α^* encompasses the critical transition density $\rho_c^* \sim 0.01\alpha^{*3}$ for a disorder-induced Anderson transition in an off-diagonally disordered tight-binding model.

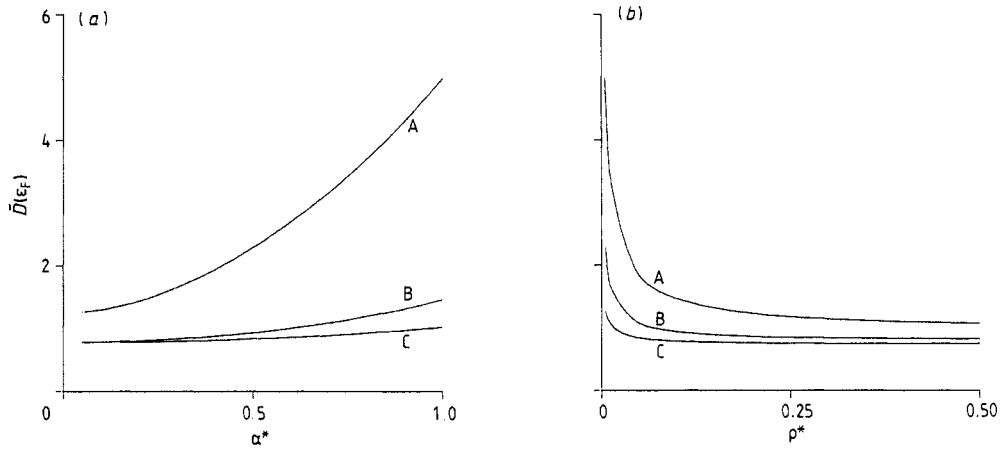

Figure 8. (*a*) The reduced density of states at the Fermi level, $\bar{D}(\varepsilon_F)$, as a function of α^* for (A) $\rho^* = 0.005$, (B) $\rho^* = 0.1$ and (C) $\rho^* = 1$. (*b*) $\bar{D}(\varepsilon_F)$ as a function of ρ^* for (A) $\alpha^* = 1$, (B) $\alpha^* = 0.5$ and (C) $\alpha^* = 0.05$.

It is known that all single-site theories for $\bar{G}(z)$ reduce to the MTA result in the limit of a completely random distribution of sites. This can be shown for the SSCA by setting $\sigma = 0$ in equations (18); this gives the condition $C^0(R) = V(R)$ for all R, which when substituted into equation (4) gives the MTA result

$$z\bar{G}(z) = 1 + \rho(\bar{G}(z))^2 \int \frac{\mathrm{d}\boldsymbol{k}}{(2\pi)^3} \frac{(\hat{V}(\boldsymbol{k}))^2}{1 - \rho\bar{G}(z)\hat{V}(\boldsymbol{k})}. \tag{32a}$$

This can be rewritten as

$$z\bar{G}(z) = 1 + \rho(\bar{G}(z))^2 \int \mathrm{d}\boldsymbol{R}\, \Phi(\boldsymbol{R}) V(-\boldsymbol{R}) \tag{32b}$$

where $\Phi(\boldsymbol{R}) \equiv \Phi(\boldsymbol{R}; \rho\bar{G}(z))$ is the inverse Fourier transform of $\hat{V}(\boldsymbol{k})[1 - \rho\bar{G}(z)\hat{V}(\boldsymbol{k})]^{-1}$. If $\Phi(\boldsymbol{R})$ were replaced by its lowest-order approximation, $V(\boldsymbol{R})$, then as discussed in I equation (32*b*) would lead to a symmetric Hubbard density of states. In this context, therefore, $\Phi(\boldsymbol{R}; \rho\bar{G}(z))$ can be regarded as an effective energy- and density-dependent transfer matrix element, the energy dependence of which leads to asymmetry in the resulting density of states (cf. Logan and Wolynes 1986).

For the Yukawa matrix element, equation (22), we have

$$\hat{V}(\boldsymbol{k}) = -4\pi V_0/(\alpha^2 + k^2) \tag{33}$$

and hence

$$\hat{\Phi}(\boldsymbol{k}; \rho\bar{G}(z)) = -4\pi V_0/(\tilde{\alpha}^2 + k^2) \tag{34a}$$

where

$$\tilde{\alpha} = [\alpha^2 + 4\pi\rho V_0 \bar{G}(z)]^{1/2}. \tag{34b}$$

Taking the inverse Fourier transform gives

$$\Phi(\boldsymbol{R}; \rho\bar{G}(z)) = -(V_0/R)\exp(-\tilde{\alpha}R). \tag{35}$$

Thus $\Phi(\boldsymbol{R})$ is also of Yukawa form but with a renormalised energy-dependent decay

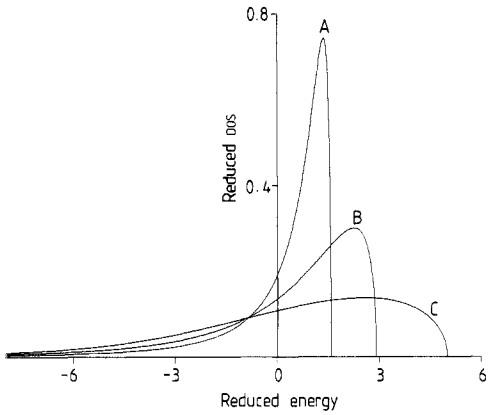

Figure 9. The reduced density of states, $D'(\varepsilon')$, obtained from the SSCA/EMA for $\rho' = 2.4$ and (A) $\alpha^* = 0.5$, (B) $\alpha^* = 0.2$, compared with (C) the perfectly random limit result ($\alpha^* = 0$) obtained from the MTA for $\rho' = 2.4$. Note the different set of units used from those used in figures 5, 6 and 7.

length $\tilde{\alpha}^{-1}$, although it must be remembered that $\tilde{\alpha}$ is complex inside the band and so $\Phi(\boldsymbol{R})$ will contain an oscillatory factor. Substituting equation (35) into (32*b*) and performing the integration shows that $\bar{G}(z)$ satisfies the cubic equation

$$4\pi\rho V_0^3(\bar{G}(z))^3 - (z^2 + 2\alpha V_0 z)(\bar{G}(z))^2 + 2(z + V_0\alpha)\bar{G}(z) - 1 = 0. \tag{36}$$

For a completely random distribution of sites, $a_H = \alpha^{-1}$ is the sole length scale in the problem. Defining the dimensionless variables

$$\rho' = \rho\alpha^{-3} \qquad z' = z/V_0' \qquad \bar{G}'(z) = V_0'\bar{G}(z) \tag{37}$$

where $V_0' = V_0\alpha$ has dimensions of energy, equation (36) reduces in the limit of real $z' = \varepsilon'$ to

$$4\pi\rho'(\bar{G}'(\varepsilon'))^3 - (\varepsilon'^2 + 2\varepsilon')(\bar{G}'(\varepsilon'))^2 + 2(\varepsilon' + 1)\bar{G}'(\varepsilon') - 1 = 0. \tag{38}$$

For energies outside the band, equation (38) has three real roots. Within the band, equation (38) has two complex-conjugate roots, and that with the negative imaginary part gives the dimensionless density of states via

$$D'(\varepsilon') \equiv V_0'D(\varepsilon') = -\pi^{-1}\,\mathrm{Im}\,\bar{G}'(\varepsilon'). \tag{39}$$

Note that by choosing that root of equation (38) with the negative imaginary part, we are implicitly taking the limit of $z' = \varepsilon' + i\eta$ as $\eta \to 0^+$ rather than as $\eta \to 0^-$.

To compare the density of states resulting from the MTA equations (38) and (39) with the previous SSCA/EMA results, we use the following expressions which interrelate the relevant variables in the two theories:

$$\rho' = \rho^*\alpha^{*-3} \qquad \varepsilon' = \varepsilon\alpha^{*-1} \qquad D'(\varepsilon') = \alpha^*\tilde{D}(\varepsilon). \tag{40}$$

Figure 9 shows the density of states $D'(\varepsilon')$ for a fixed $\rho' = \rho a_H^3 = 2.4$, and for (i) $\alpha^* = 0.5$ (curve A), (ii) $\alpha^* = 0.2$ (curve B) and (iii) $\alpha^* = 0$ (curve C). Curve C is the MTA result and curves A and B are from the SSCA/EMA, corresponding to $\rho^* = 0.3$ and $\rho^* = 0.0192$ respectively. The lower band edges occur at $\varepsilon' = -27.38$ (A), -30.37 (B) and -31.15 (C); the corresponding upper band edges occur at $\varepsilon' = 1.59$ (A), 2.92 (B) and 5.01 (C), and it is interesting to note that the inclusion of σ has a greater relative

effect on the upper band edge than on the lower edge. Figure 9 illustrates clearly the significant effect that inclusion of the hard-sphere diameter σ has upon the density of states. For example, in liquid metals that are adequately described by a tight-binding model, the mutual impenetrability of the ion cores, represented by σ, cannot be ignored and we would expect the density of states to be more like curve A than curve C. In contrast, for many doped semiconductors the effective Bohr radius, $a_H = \alpha^{-1}$, of the impurity species is much greater than σ, giving a low value of α^* and hence a more diffuse density of states. To obtain an adequate representation of the density of states for a particular system of interest, care must clearly be taken to include the appropriate value of σ.

5. Discussion

In the preceding sections we have developed an analytic solution to the SSCA/EMA for a Yukawa transfer matrix element, and for the simple case of a step function pair distribution function. This yielded a quartic equation, (30), for the self-energy which was solved to give the configurationally averaged diagonal Green function and hence the density of states. It is known that the EMA is the most accurate theory for the density of states of spatially disordered systems at higher densities (see e.g. Roth 1976, Aloisio *et al* 1981), but the EMA has also been regarded as more difficult to implement computationally than other less accurate single-site theories such as those of Ishida and Yonezawa (1973) and Movaghar and Miller (1975). As we have discussed, however, the EMA and the SSCA are equivalent, and can be solved analytically for the case $g_2(R) = \theta(R - \sigma)$, and for a wide variety of transfer matrix elements of which a Yukawa is probably the simplest. Moreover, liquid-state techniques are available whereby the OZ form, equation (3), with the closure relation, (12), may be solved numerically for a more realistic pair distribution function.

We also add that, although our primary interest has been in the averaged diagonal Green function, the theory also yields the averaged off-diagonal Green function, $\bar{G}(12) \equiv \bar{G}(\boldsymbol{R})$. The latter, once $\bar{G}(z)$ and $S(z)$ are known from equations (29) and (30), can readily be obtained from equations (3), (6), (18*b*) and (23). The electrical conductivity of the disordered system is related to the configurational average of a product of two (in general) off-diagonal Green functions (Matsubara and Toyozawa 1961). In the limit of weak disorder (the Boltzmann regime) this average can be broken, and approximated as a product of averaged Green functions; hence, with $\bar{G}(z)$ and $\bar{G}(\boldsymbol{R})$ known, we can calculate the electrical conductivity. This approach is of course valid only at high enough densities where the electronic states are sufficiently extended that scattering due to the disorder can be described by a Boltzmann equation. This is also the density region in which we expect the SSCA/EMA to yield an accurate description of the averaged Green functions required to calculate the Boltzmann conductivity.

We now discuss briefly some possible extensions of the theory developed in this paper. As was mentioned in § 1 (and discussed in detail in I), inclusion of site-diagonal disorder is straightforward for any single-site theory, with the site energies regarded as independent random variables with a given normalised probability distribution $P(\varepsilon_i)$. As shown in I, the single-site averaged diagonal Green function, averaged over all configurations and site energies, is determined from

$$\bar{G}(z) = \int_{-\infty}^{\infty} \mathrm{d}\varepsilon_i \frac{P(\varepsilon_i)}{z - \varepsilon_i - S(z)}. \tag{41}$$

Here $S(z) \equiv S(\bar{G}(z))$ is the single-site self-energy, which is *independent* of ε_i and, if viewed as a function of $\bar{G}(z)$, is identical to the self-energy in the *absence* of diagonal disorder (equation (24*a*)); for the case of the SSCA/EMA with $g_2(R) = \theta(R - \sigma)$ and Yukawa $V(R)$, this is precisely the $S(\bar{G}(z))$ obtained from equation (26). Therefore, given a form for $P(\varepsilon_i)$, we can obtain $\bar{G}(z)$ (and hence the density of states) in the presence of site-diagonal disorder, once we know $S(\bar{G}(z))$ in the absence of diagonal disorder. A particularly simple example occurs when ε_i has a Lorentzian distribution

$$P(\varepsilon_i) = \gamma\pi^{-1}/(\gamma^2 + \varepsilon_i^2) \tag{42}$$

with a halfwidth γ. This may be used to model inhomogeneous broadening effects relevant, for example, to the impurity band of a doped and compensated semiconductor, or to the case of electronic excitons, where γ may be density- and temperature-dependent. Equations (42) and (41) combine to yield

$$(z + \mathrm{i}\gamma)\bar{G}(z) = 1 + \bar{G}(z)S(z) \tag{43}$$

for $\operatorname{Im} z > 0$. Comparison with equation (25) shows that the effect of including Lorentzian site disorder is simply equivalent to moving z into the complex plane by an amount $\mathrm{i}\gamma$. For the SSCA/EMA Yukawa problem discussed in § 3, a simple replacement of $\tilde{z} = \varepsilon + \mathrm{i}0^+$ by $\tilde{z} = \varepsilon + \mathrm{i}\tilde{\gamma}$ ($\tilde{\gamma} = \gamma/V_0^*$) in equation (30) yields the appropriate $S(z)$ which, when combined with equation (43), gives $\bar{G}(z)$ for the case of Lorentzian site disorder.

Another physical effect that is readily included is that of excitation loss mechanisms from a site, such as radiative decay processes (e.g. fluorescence or phosphorescence) relevant to electronic excitations. Such processes are incorporated simply by setting $z = E + \mathrm{i}\eta$, where η is finite and corresponds essentially to an inverse radiative decay time. The inclusion of loss mechanisms characterised by a finite η is obviously mathematically equivalent to including Lorentzian site disorder in a single-site theory. If both effects are present, then the single-site $\bar{G}(z)$ will be given via equation (43) with $z = E + \mathrm{i}\eta$. In the limit of weak inter-site coupling (small V_0 and/or ρ) it is clear from equations (43) and (24*a*) that the resultant density of states, $D(E) = -\pi^{-1} \operatorname{Im} \bar{G}(E + \mathrm{i}\eta)$, tends to a Lorentzian form with a half-width of $\eta + \gamma$ arising from a combination of static (inhomogeneous broadening) and dynamical (loss) effects. The subsequent evolution of $D(E)$ with increasing density is determined as described above.

One defect of the SSCA/EMA, which it shares with all other single-site theories, is that it does not give a correct description of the density of states at number densities sufficiently low that multiple-hopping processes between sites (described by non-single-site graphs) become important. Another improvement to the theory presented here would therefore be to include additional pair-site graphs in $C^0(12)$. This can be achieved via an alternative closure relation to the OZ analogue equation, (11); for example,

$$H^0(12) = \frac{g_2(12)V(12)}{1 - (\bar{G}(z)V(12))^2} + g_2(12)(H^0(12) - C^0(12)) \tag{44}$$

where we assume for convenience that $V(12) = V(21)$. This is similar to the SSCA closure relation, (13), except for a more complex $\tilde{C}^0(12)$ term which describes all multiple-hopping processes between a pair of sites. The second term on the right-hand side of equation (44) depends explicitly on density (see equation (11)), and so at low densities the first term will clearly dominate. If we therefore neglect the second term

and substitute equation (44) into equation (2), we obtain the correct low-density limit of the self-consistency equation for $\bar{G}(z)$, as derived by Elyutin (1981) for the case $g_2(R) = 1$:

$$z\bar{G}(z) = 1 + \rho(\bar{G}(z))^2 \int \mathrm{d}\boldsymbol{R} \frac{g_2(\boldsymbol{R})(V(\boldsymbol{R}))^2}{1-(\bar{G}(z)V(\boldsymbol{R}))^2}. \tag{45}$$

The density of states resulting from equation (45) at low values of ρ has been discussed in some detail in I (see also Gibbons *et al* 1988). If, on the other hand, we approximate the first term on the right-hand side of equation (44) by its leading term, $g_2(12)V(12)$, we recover the SSCA result. The closure equation (44) thus leads to an SSCA-like theory with the additional advantage that it reduces to the correct low-density limit, unlike true single-site theories. This approach is similar in spirit to that of Tsukada (1974) and Whitelaw and McLaughlin (1979), except that these authors have introduced the somewhat artificial idea of enclosing a pair of sites inside a sphere, and treating differently the self-energy contributions from inside and outside the sphere.

In general, equation (11) with the closure relation (44) may be solved numerically to give $H^0(12)$ as a function of $\bar{G}(z)$, insertion of which into equation (2) yields a self-consistency equation for $\bar{G}(z)$. To proceed analytically, however, it is convenient to consider again the simple pair distribution function $g_2(R) = \theta(R-\sigma)$. Coupled with equation (44), this yields the two closure relations

$$\begin{aligned} &H^0(R) = 0 && :R < \sigma \\ &C^0(R) = \{V(R)/[1-(\bar{G}(z)V(R))^2]\} && :R > \sigma \end{aligned} \tag{46}$$

which, like equations (18), resemble the MSA closure conditions (21) and (20*b*), but for a more complicated potential. The simplest case would be to take $V(R)$ constant and finite over a range $\sigma < R < L$, and zero for $R > L$, and to use Perram's (1983) method to obtain a solution to the OZ analogue equation, (11). Although this is a simplistic transfer matrix element, it may be sufficient to assess the importance of including multiple-hopping processes between pairs of sites; see also Whitelaw and McLaughlin (1979) who have incorporated multiple-hopping effects in a one-dimensional tight-binding model.

Finally, we comment on inclusion of overlap in the model. It has been implicitly assumed that the site orbitals form an orthonormal set. Relaxation of the orthogonality assumption is, however, achieved simply by replacing the transfer matrix element V_{ij} with an effective energy-dependent transfer matrix element $\tilde{V}_{ij} = V_{ij} - (z-\varepsilon_j)S_{ij}$, where $S_{ij} \equiv S(\boldsymbol{R}_{ij})$ is the overlap integral between orbitals on sites i and j. For pure off-diagonal disorder ($\varepsilon_j = 0$ for all j), and with V_{ij} replaced by $V_{ij} - zS_{ij}$, the analysis of §§ 1 and 2 is applicable to this case. It should, however, be noted that $C(12)$, expressed in strongly irreducible form, now depends explicitly on the energy variable z through the energy dependence of $\tilde{V}_{ij}$; in contrast to the case of orthogonal orbitals considered previously, the right-hand side of the self-consistency equation, (4), thus depends explicitly on z. The effects of including overlap in the EMA have been studied numerically (e.g. Roth 1976) for the case in which the overlap integral, $S(R)$, and the transfer matrix element, $V(R)$, have the same R-dependence. For the Yukawa transfer matrix element, equation (22), and with $V(R) = \lambda S(R)$, overlap effects are readily incorporated into the analytic solution of the SSCA/EMA described in § 3, by replacing V_0 with $V_0[1 - z/\lambda]$.

Acknowledgment

MDW is grateful for the award of a SERC postgraduate studentship.

References

Aloisio M, Singh V A and Roth L M 1981 *J. Phys. F: Met. Phys.* **11** 1823–32
Baxter R J 1968 *Aust. J. Phys.* **21** 563–9
Chandler D, Schweizer K S and Wolynes P G 1982 *Phys. Rev. Lett.* **49** 1100–3
Elyutin P V 1981 *J. Phys. C: Solid State Phys.* **14** 1435–43
Gibbons M K, Logan D E and Madden P A 1988 *Phys. Rev.* B **38** 7292–302
Hall R W and Wolynes P G 1985 *J. Chem. Phys.* **83** 3214–21
Hansen J P and McDonald I R 1986 *Theory of Simple Liquids* (New York: Academic)
Høye J S and Blum L 1977 *J. Stat. Phys.* **16** 399–413
Høye J S and Olaussen K 1982 *J. Chem. Phys.* **77** 2583–6
Høye J S and Stell G 1976 *Mol. Phys.* **32** 195–207
—— 1981 *J. Chem. Phys.* **75** 5133–42
Høye J S, Stell G and Waisman E 1976 *Mol. Phys.* **32** 209–30
Ishida Y and Yonezawa F 1973 *Prog. Theor. Phys.* **40** 731–53
Katz I and Rice S A 1972 *J. Phys. C: Solid State Phys.* **5** 1165–82
Lebowitz J L and Percus J K 1966 *Phys. Rev.* **144** 251–8
Logan D E 1984 *Mol. Phys.* **51** 1365–94, 1395–417
Logan D E and Winn M D 1988 *J. Phys. C: Solid State Phys.* **21** 5773–95
Logan D E and Wolynes P G 1986 *J. Chem. Phys.* **85** 937–48
Matsubara T and Toyozawa Y 1961 *Prog. Theor. Phys.* **26** 739–56
Movaghar B and Miller D E 1975 *J. Phys. F: Met. Phys.* **5** 261–76
Perram J W 1983 *Molec. Phys.* **49** 461–73
Roth L M 1974a *J. Physique* **35** C4 317–23
—— 1974b *Phys. Rev.* B **9** 2476–84
—— 1975 *Phys. Rev.* B **11** 3769–79
—— 1976 *J. Phys. F: Met. Phys.* **6** 2267–88
Schweizer K S 1986 *J. Chem. Phys.* **85** 4638–49
Schweizer K S and Chandler D 1983 *J. Chem. Phys.* **78** 4118–25
Smith E R 1979 *Mol. Phys.* **38** 823–41
Thompson M J, Schweizer K S and Chandler D 1982 *J. Chem. Phys.* **76** 1128–35
Tsukada M 1974 *J. Phys. C: Solid State Phys.* **7** 1475–90
Waisman E 1973 *Mol. Phys.* **25** 45–8
Waisman E and Lebowitz J L 1970 *J. Chem. Phys.* **52** 4307–9
Wertheim M S 1963 *Phys. Rev. Lett.* **10** 321–3
—— 1971 *J. Chem. Phys.* **55** 4291–8
—— 1973 *Mol. Phys.* **25** 211–23
Whitelaw D J and McLaughlin I L 1979 *J. Phys. C: Solid State Phys.* **12** 3217–26
Yonezawa F, Roth L M and Watabe M 1975 *J. Phys. F: Met. Phys.* **5** 435–42